A&A manuscript no.
(will be inserted by hand later)

Your thesaurus codes are:
08 (08.02.1; 08.02.4; 08.14.2; 08.09.2; 13.25.5; 02.13.1)

ASTRONOMY AND ASTROPHYSICS

February 1, 2008

The New AM Her System RX J0704.2+6203

Northern Twin of BL Hyi

G. H. Tovmassian[1], P. Szkody[2⋆], J. Greiner[3], S.V. Zharikov[1], F.-J. Zickgraf[4], A. Serrano[5], J. Krautter[6], I. Thiering[6], and V. Neustroev[7⋆⋆]

[1] OAN, Instituto de Astronomía,UNAM, México
email: gag@astrosen.unam.mx
[2] Department of Astronomy, Box 351580, University of Washington, Seattle, USA
email: szkody@astro.washington.edu
[3] Astrophysical Institute Potsdam, An der Sternwarte 16, 14482 Potsdam, Germany
email: jgreiner@aip.de
[4] Observatoire Astronomique de Strasbourg, France
[5] Instituto Nacional de Astrofísica Optica y Electrónica, AP 51 y 216, Puebla, Pue., México
[6] Landessternwarte Königstuhl, 69117 Heidelberg, Germany
[7] Udmurtia State University, Universitetskaya st., Izhevsk, Russia

Received ; accepted

Abstract. We report here on the identification and study of the optical counterpart of the ROSAT source RX J0704.2+6203. Extensive spectral and photometric observation showed that the object belongs to the class of magnetic Cataclysmic Variables. We determined the orbital period of the system to be $97\overset{\mathrm{m}}{.}27$ and estimated the strength of its magnetic field to be on the order of 20 MG. The system was observed in both high and low states, common for its class. Other parameters of the magnetic close binary system were estimated. The spectral and photometric behavior of the object is similar to that of the well studied polar BL Hyi.

Key words: stars: cataclysmic variables – stars: individual: RX J0704.2+6203 – stars: magnetic field – binaries: close – X-rays: stars – accretion

1. Introduction

As part of a program devoted to the optical identification of a complete sample of northern ROSAT all-sky survey (RASS) X-ray sources, we identified a new magnetic cataclysmic variable (CV). Since October 1991 nearly 800 X-ray sources have been observed within the identification program[1]. A detailed description of the project is given by Zickgraf et al. (1997). Here we report the identification and detailed follow-up observations of the optical counterpart of the ROSAT all-sky survey X-ray source RX J0704.2+6203 (= 1 RX J070409.2+620330). It is the fourth magnetic cataclysmic Variable (CV) discovered within this collaboration (Tovmassian et al. 1998, 1999, 2000).

Magnetic CVs (Polars) are close interacting double systems comprised of a white dwarf (WD) and a pre-main sequence red dwarf, in which the accretion of matter onto the WD is governed by its strong magnetic field. Instead of forming an accretion disc, as common in most other CVs, matter is funneled to the magnetic pole on the WD through the magnetic lines. A standoff shock forms near the surface of the WD. The shocked plasma cools through bremstrahlung and cyclotron radiation as it settles onto the WD (Warner 1995). Polars tend to cluster below the "period-gap", i.e. periods less than 2 hours, and they often exhibit characteristic light curves, spectral distribution and profiles of emission lines easily distinguishable from other types of CVs. BL Hyi is one of the well studied examples of a polar. We found a number of similarities in behavior and the parameters of RX J0704.2+6203 with those of the well studied BL Hyi. Here we report our observations and findings on this newly discovered magnetic CV.

Send offprint requests to: G. Tovmassian,
P.O.Box 439027, San Diego, CA 92143, USA

⋆ Based on observations with the Apache Point Observatory (APO) 3.5 m telescope, which is owned and operated by the Astrophysical Research Consortium (ARC)

⋆⋆ Special Astron. Obs., 357147 Nizhnij Arkyz, Russia

[1] The identification project is a collaboration of the Max-Planck-Institut für extraterrestrische Physik, Garching, Germany, the Landessternwarte Heidelberg (LSW), Germany, and the Instituto Nacional de Astrofisica, Optica y Electronica (INAOE), Puebla, Tonantzintla, Mexico.

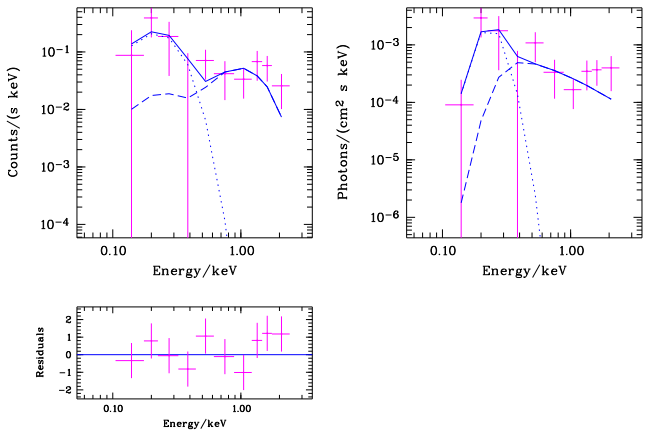

Fig. 1. ROSAT PSPC X-ray spectrum of RX J1554.2+2721 as derived from the all-sky survey data, fitted with a sum of a blackbody and a thermal bremsstrahlung model. The lower left panel shows the deviation between data and model in units of χ^2 per bin.

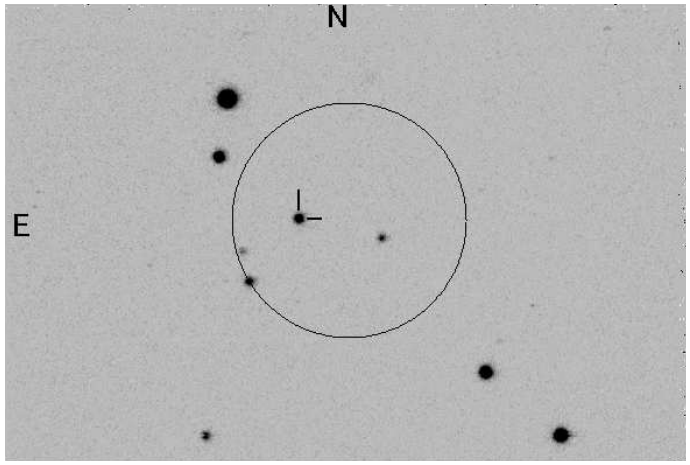

Fig. 2. The CCD images of the RX J0704.2+6203 in R_c band from SAO RAS 1^{m}telescope. The object in a high luminosity state at the maximum of the light curve is marked. The corresponding ROSAT error box is also marked.

2. Observations

2.1. X-ray observations

RX J0704.2+6203 ≡ 1RXS J070409.2+620330 was scanned during the ROSAT all-sky-survey over a period of 2.5 days in Sep. 20-23, 1990 for a total observing time of 340 sec. Its mean count rate in the ROSAT position-sensitive proportional counter (PSPC) was 0.13 cts/s, and the hardness ratio $HR1 = -0.00 \pm 0.15$ where $HR1$ is defined as (H–S)/(H+S), with H (S) being the counts above (below) 0.4 keV over the full PSPC range of 0.1–2.4 keV. Thus, the X-ray spectrum is comparatively hard. Despite the small number of counts a fit with a one-component model, like a pure blackbody model, is not acceptable. Applying a sum of a black body and a thermal bremsstrahlung model with the temperature of the latter component fixed to 20 keV (it is not constrained at all by the ROSAT data) gives a good reduced $\chi^2 = 1.04$ (see Fig. 1) and the following fit parameters: $kT_{\rm bbdy} = 19\pm15$ eV, $N_{\rm H} = 3.1\times10^{21}$ cm^{-2}. For a better comparison to the parameters of similar sources we also fixed the black body temperature to $kT_{\rm bbdy} = 25$ eV, and derive $N_{\rm H} = 4.5\times10^{20}$ cm^{-2}, Norm$_{\rm bbdy} = 0.23$ and Norm$_{\rm thbr} = 3.0\times10^{-4}$. This gives an unabsorbed 0.1–2.4 keV flux of 1.1×10^{-11} erg cm^{-2} s^{-1} (or 2.9×10^{-11} erg cm^{-2} s^{-1} bolometric), corresponding to an unabsorbed bolometric luminosity of 3.5×10^{31} (D/100 pc)^2 erg s^{-1}.

2.2. Optical observations

The optical counterpart was identified on the 2.1m telescope with the faint object spectrograph (LFOSC, Zickgraf et al. 1997) at Guillermo Haro Observatory, Cananea, Mexico (Appenzeller et al. 1998). The finding chart of RX J0704.2+6203 is presented in Fig.2 with the ROSAT 30″error box marked. The object was caught in both high (Fig.2) and low states, common to Polars. The coordinates of the object derived from POSS are
RA= 07^h 04^m 09.″9 DEC=+62°03′27″ Eq.=2000.

RX J0704.2+6203 was confirmed as a CV with a few higher-resolution spectra obtained at the 2.1m telescope of Observatorio Astronómico Nacional de San Pedro Mártir (OAN SPM) in Mexico. The Boller & Chivens spectrograph with moderate $4-5$ Å FWHM resolution was used. But the faintness of the object prevented us from obtaining a set of data with sufficient time resolution. Using the same telescope with the f/13.5 secondary focus of the 2.1 m telescope (instead of f/7.5 as used for spectroscopy), infrared J band photometry of the object, covering multiple orbital periods was accomplished on Nov 24, 1998. The Camila IR camera operating NICMOS3 256 × 256 detector sensitive from 1 to 2.5 microns was used. IR standard objects were observed for magnitude calibration.

RX J0704.2+6203 was observed extensively at the 1m telescope Zeiss-1000 of the Special Astrophysical Observatory of Russian Academy of Sciences (SAO RAS) with the CCD in Johnson-Kron-Cousins photometric BVRcIc system. In total, the observations span a long baseline of several years. Here, again, we observed standard fields in order to not only perform differential photometry, but also calculate the visual magnitudes of the object. The log of these and all other optical observations is presented in Table 1.

Observations with low spectral resolution were obtained using the long slit spectrograph (UAGS) at the prime focus of the 6 m telescope of SAO RAS on Nov 04

& 05 1999. The data were obtained with ≈ 10 Å FWHM resolution in the $3630-8340$ Å spectral range. These spectra were flux calibrated using spectrophotometric standard star observation during the same nights and were instrumental for the study of the continuum flux distribution.

Higher spectral resolution observations of RX J0704.2+6203 were performed on the 3.5 m telescope at Apache Point Observatory The double-imaging spectrograph (DIS) was used in the two wavelength regions 4200-5100 and 5800-6800 Å to obtain a set of medium-high-spectral resolution (FWHM 2.5 Å) and high-time resolution ($0.1\,P_{orb}$) spectra covering almost two orbital periods. Once again we observed spectrophotometric standards for flux calibration.

Both spectral and photometric observations were reduced with IRAF[2] packages.

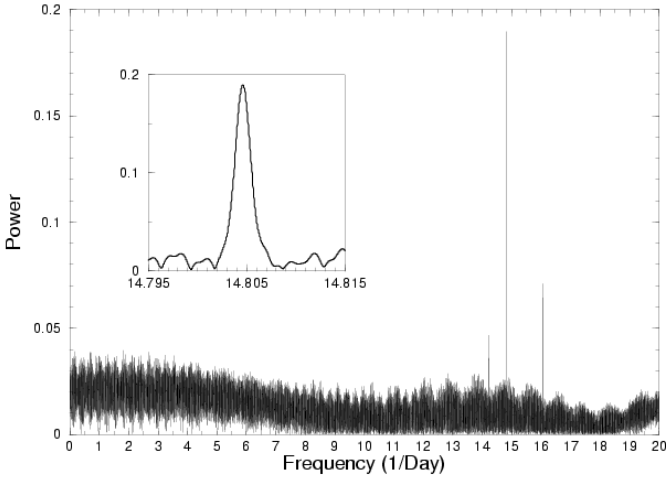

Fig. 3. The CLEANed power spectrum. In the inset the highest peak of the power spectrum is zoomed up.

3. The Orbital Period

3.1. Photometric

The orbital period of the system was determined based on the full set of observations that we collected over 3 years. The light curves in the different bands and in the different luminosity states were all normalized to the same minimum level. These also include fluxes derived from the spectral observations. The light curves all display distinct hump structure with varying amplitude depending on wavelength and luminosity state. This feature served for period determination almost as well as an eclipse does in high–inclination systems. Thus, we were able to derive the orbital period from photometry with high precision.

We used discrete Fourier transformation techniques for our period search, combined with the CLEAN procedure (Roberts et al. 1987), which basically deconvolves the window function with the actual power spectrum in order to depress spectral peaks originating from the temporal distribution of the data. We first calculated the power spectra of sufficiently long individual data sets. They all were consistent with each other in showing the maximum peak in the power spectral distribution at around $0\overset{d}{.}0675$. Finally we performed the analysis on the combined set of data.

Figure 3 presents the CLEANed power spectrum of the combined data. The strongest peak corresponds to the value obtained previously from the separate sets of data. The strength and narrowness of the single peak (see the inset of the figure for the zoomed up profile of the central peak) shows the coherence of the periodic signal in the data comprised of measurements at different wavelengths and even at different luminosity states of the object. Our estimate is accurate to 0.007 minutes. According to our analysis the orbital period of RX J0704.2+6203 is Porb=0.06754658+/-0.000005 days = 97.2671 min.

3.2. Spectroscopic

After we had a photometric period, we could determine the spectroscopic period of the system for comparison. We used the set of higher resolution spectra obtained at the APO 3.5 m telescope for that purpose.

We used the two strongest lines in the spectrum of RX J0704.2+6203 (Hβ and He II). Analysis of the profiles of these emission lines has been shown to be an efficient way to distinguish the various emission components that are present in magnetic CVs. A brief examination of the line profiles and constrained two–dimensional images (trailed spectra) showed that there is a dominant component of the emission lines in both the Balmer and ionized Helium lines. Thus, it was relatively simple to disentangle it from the underlying fainter component(s) by simple deblending the line with two Gaussians. As soon as we had line centers determined for the dominant component of the emission lines it was easy to fit them with a regular *sin* curve with the period determined from photometry. Then the re-calculated values of line centers of that component from the fit were used for a second iteration of deblending, with one Gaussian fixed at the calculated wavelength, to refine the parameters of the second component. Although some polars show more than two components in the emission lines, in this case, we reached a satisfactory fit and could not find any evidence of additional sources. Usually two prominent components are easily distinguishable. They are narrow emission line (NEL) component originating from irradiated secondary, and high velocity

[2] IRAF is the Image Reduction and Analysis Facility, a general purpose software system for the reduction and analysis of astronomical data. IRAF is written and supported by the IRAF programming group at the National Optical Astronomy Observatories (NOAO) in Tucson, Arizona. NOAO is operated by the Association of Universities for Research in Astronomy (AURA), Inc. under cooperative agreement with the National Science Foundation

Table 1. The Log of Optical Observations

Date UT	JD	Telescope + Equip.	Filter/Wvlngth	Duration min.	Exp. sec.	Site
1997 March 03	2450510	2.1m, B&Ch+CCD	3600–6200	120	1200	SPM
1997 November 01	2450754	1.0m, CCD	R	240	600	SAO
1997 November 02	2450755	1.0m, CCD	R	200	600	SAO
1998 January 03	2450817	1.0m, CCD	R	140	600	SAO
1998 February 27	2450872	1.0m, CCD	R	325	600/300	SAO
1998 February 28	2450873	1.0m, CCD	R	185	480/300	SAO
1998 March 19	2450891	2.1m, B&Ch+CCD	4100–6700	120	600/900	SPM
1998 November 24	2451141	2.1m, Camila	J	270	40	SPM
1998 November 24	2451141	3.5m, DIS	4240–5060; 5795–6835	165	600	APO
1999 January 12	2451191	1.0m, CCD	V I	285	500/240	SAO
1999 January 16	2451194	1.0m, CCD	R	210	600/300	SAO
1999 January 16	2451194	1.0m, CCD	B	25	600/300	SAO
1999 November 04	2451487	6.0m,UAGS+CCD	3630–8370	125	600	SAO
1999 November 05	2451488	6.0m,UAGS+CCD	3630–8370	180	600	SAO

component (HVC) which probably emitted by the stream of matter free-falling from the inner L_1 point toward the WD. The former has FWHM about 2.5 Å or less, it may reach up to 400 km/sec semi-amplitude of radial velocity in high-inclination, eclipsing systems, and its flux is significantly higher at around 0.5 orbital phase, when it is behind WD and faces observer with heated side of its surface. While the latter, due to the gradient of intrinsic velocities inside the stream is broader and fuzzy (usually about 7-8 Å) reaching up to 1500 km/sec in higher inclination systems, but can be much lower in others. HVC reaches maximum positive velocity at around orbital phase zero (see Schwope et al. (1999) and references therein for description of components of emission lines). Emitting area of HVC is less compact and corresponding component in lines of different excitation levels may have differing phase and semi-amplitude of radial velocities.

Thus, the RV of emission lines were successfully separated into two components shown with different symbols in Figure 4. Both are modulated with the photometric orbital period. Both show a relatively large amplitude of radial velocity variation. The component drawn by filled squares is very distinct and is well described by

$$V_{em} = \gamma + K_{em1} \sin(2\pi(t - t_0)/P_{\rm orb})$$

We obtained K_{em1}= 387 and 422 km/sec for Hβ and He II respectively. The phase shift of 0.06 P_{orb} between same component of two different lines is remarkable in the sense that, the high values of K_{em1} combined with the phase shift between lines of various excitation in a relatively low–inclination system (absence of eclipses), indicates that this component of the emission line probably originates in the stream. Our designation of this component as pertaining to the stream (HVC) in spite of its relatively low amplitude is further supported by Doppler tomography (see below).

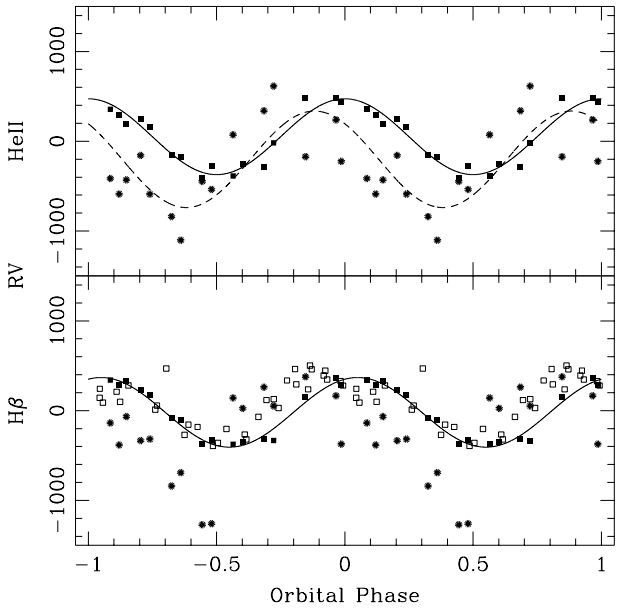

Fig. 4. The radial velocity curves. On the lower panel measurements of Hβ emission line components are presented. The stronger and better defined component marked by filled squares is described by solid *sin* curve. The second component supposedly from the magnetic part of the stream is marked by asterisks. The open squares are measurements of the whole line on low resolution spectra. On the upper panel the measurements of both components of He II line are presented with corresponding fits.

The other curve, marked by a dashed line fitted to the second component of the emission lines, is not as well defined. This component fitted with a sin curve with semi-amplitude of 540 km/sec supposedly also comes from the

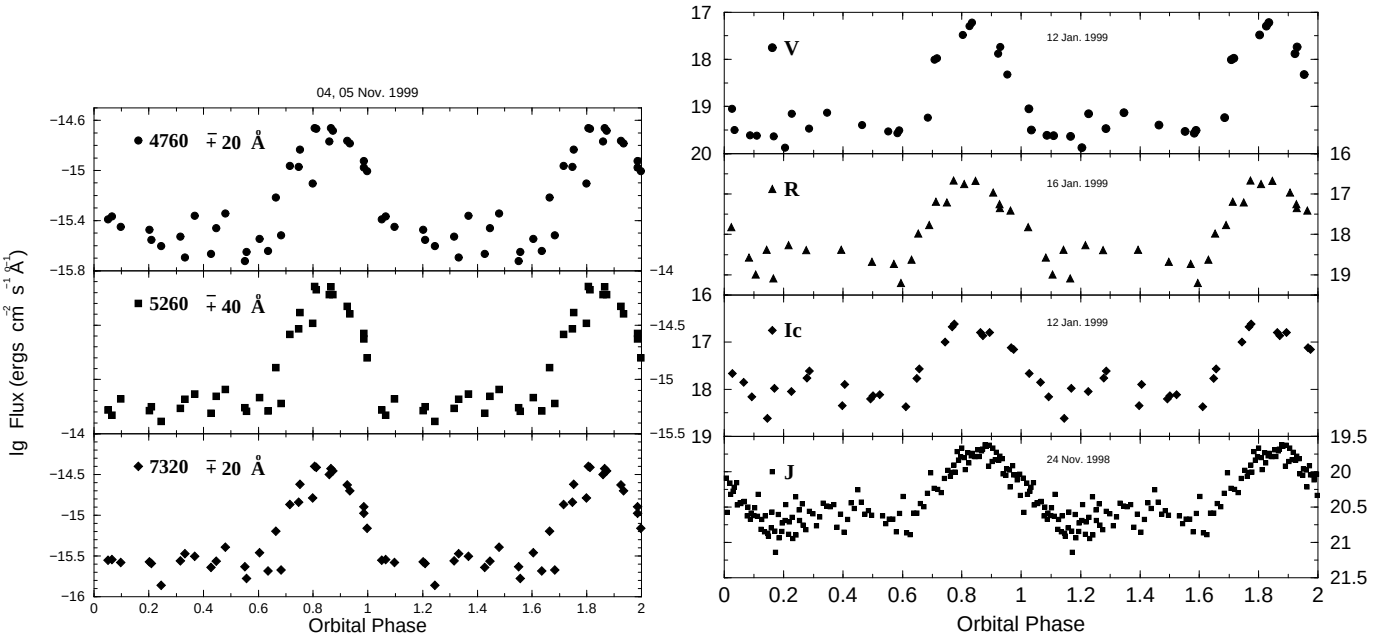

Fig. 5. The light curves of RX J0704.2+6203 in high luminosity state obtained at various epochs in different bands (as marked in the panels). The left panel displays those measured from spectrphotometry in narrow strips of continual spectrum. The fluxes in log scale are marked on vertical axes. The broad band photometry presented on right panel are in magnitudes.

stream, but from the magnetically controlled part. Open squares are measurements of the unblended emission line in the low resolution spectra. They bear signs of both components with predominant influence of the stronger and lower velocity component. We present these measurements in order to show how good the observations, that are separated by a large time gap, fold together with the orbital period determined from the photometry. Note that radial velocity variations are caused by the matter orbiting in the binary system frame, while humps in the light curve arise from the magnetic pole spinning with WD. Therefore, the coincidence of the photometric and spectroscopic periods provides good evidence of synchronized rotation of the WD in the system i.e. a polar.

4. The nature of the object and its behavior

4.1. Photometric characteristics

The light curves of RX J0704.2+6203 folded with the orbital period in different bands are presented in Figure 5. They include light curves derived from spectrophotometric observations by measuring flux in narrow bands (upper panels) as well as broad-band CCD photometry (lower).

The light curves exhibit prominent humps that vary insignificantly in amplitude from band to band and are almost identical in shape. Although the large number of sub-classes of CVs display a large range of light curves due to the numerous sources of radiation, there are easily distinguishable shapes depending on particular affiliation to one or another class. The humps in the light curve of RX J0704.2+6203 are typical of those due to a large contribution of cyclotron radiation being beamed from the accretion column. The shape and duration of the humps suggests that the spot is being eclipsed by the WD itself in its synchronized rotation with the binary period. The hump duration is about 0.6 P_{orb}. There is some indication of a secondary peak at phase 1.4, which may be attributed to the presence of the second weak accretion pole in the system. The light curve is remarkably similar to that of BL Hyi (Wolff et al. 1995).

RX J0704.2+6203 was observed in R_c band in a high luminosity state as well as in a low state. The phase folded light curve in the low state is presented in Figure 6 along with the high state light curve in the same filter for comparison. Interestingly, the light curve shape in the low state remains remarkably similar to the shape in high state. However, the amplitude of the cyclotron humps in the low state is a factor of two less than the in high state.

4.2. Spectrophotometric characteristics

The low resolution spectra of RX J0704.2+6203 obtained at the 6m telescope SAO RAS were used for a study of the continuum variation over the orbital period. As can be seen from flux measurements in narrow bands covering the continuum spectrum in Fig.5, the spectrum undergoes large changes in the course of the orbit. It can be better demonstrated by comparison of the averaged spectrum

of RX J0704.2+6203 at the maximum of the light curve humps with the averaged spectrum at the bottom (see Fig. 7. There is an enormous change in shape of the spectra, confirmed by the multiwavelength photometry also shown in the Figure.

Besides the usual set of Balmer and He lines in emission common for CVs, the spectrum at the maximum of the light curve shows a steep increase in the blue and small humps in the red. No traces of lines from the secondary could be found. Change of shape of the spectrum and continuum humps are common for magnetic CVs. Similar spectral changes were observed in another magnetic CV recently reported by Tovmassian et al. (2000). Particularly, the spectra of RX J0704.2+6203 very much resembles those of the well studied BL Hyi (Schwope et al. 1995).

The humps seen in the continuum of magnetic CVs are actually lines of cyclotron emission emitted from the magnetic column of matter accreting onto the magnetic pole of the WD in the binary system. The cyclotron emission originates in the column of in-falling matter above the magnetic pole, where it slows down and heats up before settling on the surface of the WD. It is emitted in a wide range of wavelengths from the near UV to the infrared region. Since cyclotron radiation is beamed perpendicular to the magnetic lines and since the WD is locked by its magnetic field in a synchronous rotation with the binary system, we see periodic maxima in the light curve and cyclotron spectrum appear and disappear depending on the viewing angle of the magnetic pole of the WD.

In order to separate the bulk of cyclotron emission from the rest of the emitting sources and estimate the strength of the magnetic field, the averaged spectrum at the minimum was subtracted from the spectrum at the maximum of the light curve. The spectra were shifted according to radial velocity measurements corresponding to the orbital motion. The residual spectrum is presented in Figure 8. The lines are clearly gone, thus their contribution to the luminosity change is negligible. The continuum bears apparent signs of cyclotron lines seen as humps.

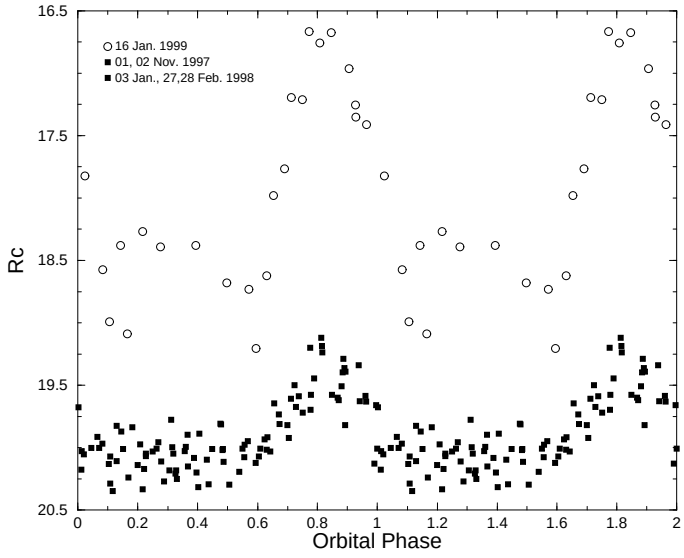

Fig. 6. The light curve of RX J0704.2+6203 in low luminosity state (filled symbols). For comparison high state light curve is repeated by open circles. Corresponding epochs are indicted in the figure.

We used the theory developed by Chanmugam & Dulk (1981), Wickramasinghe & Meggitt (1985) to constrain our models in order to describe the observed differential flux of RX J0704.2+6203 assuming its cyclotron nature. Similar models were applied by Schwope et al. (1995) and Ferrario et al. (1996) to estimate the magnetic field of the WD in BL Hyi. We calculated a set of models for emission cyclotron spectra that rises from the slab of plasma representing the post-shock region of the accretion column to fit our observations. We took the simplest view assuming a homogeneously emitting plasma.

Assuming a typical value of the order of the shock temperature for $kT = 20$ keV the observed cyclotron lines in the red portion of the spectrum can be identified as 8,7 & 6 harmonics (corresponding to peaks at $\approx$ 7450, 6600 & 5950 Å) of cyclotron emission, thus leading to a moderate 20 MG magnetic field strength. Since cyclotron emission is described by a number of parameters (temperature kT, the polar angle between the line of sight and the magnetic field θ, the field strength B and a plasma parameter $\Lambda = ln_e/B$, where l is geometric size, n_e – electron density, (Wickramasinghe & Meggitt 1985), there is some ambiguity of chosen parameters and they can be traded against each other (e.g., lower values of B and T require higher values of Λ in order to shift the cyclotron peak to the observed value and vice verse). Alternatively, the observed lines could be 9,8 & 7 harmonics (a shift by one), which will require lower value of $kT = 10$ keV in order to successfully fit the cyclotron spectrum, which in turn will lead to an increment of the magnetic field up to 24 MG. The difference is not significant, taking into account the much wider range of magnetic fields observed in mCVs. The suggested rather low value of the magnetic field strength is supported by the relatively hard X-ray spectrum typically found in low-field polars (Beuermann & Burwitz 1995; Schwope 1996).

Meanwhile, the thick straight line in the Fig.8 is a linear fit to the differential energy distribution between the maximum and minimum of the light curve, derived from photometry. It extends beyond the optical range thanks to our measurements in near IR-band J. Its steepness is an additional confirmation of the cyclotron nature of the observed radiation.

Thus, our tentative classification of RX J0704.2+6203 as a member of AM Her class of magnetic Cataclysmic Variables based on the shape of the lightcurve, presence of significant X-ray radiation and strong He II line, characteristic profiles of emission lines and the semiamplitude

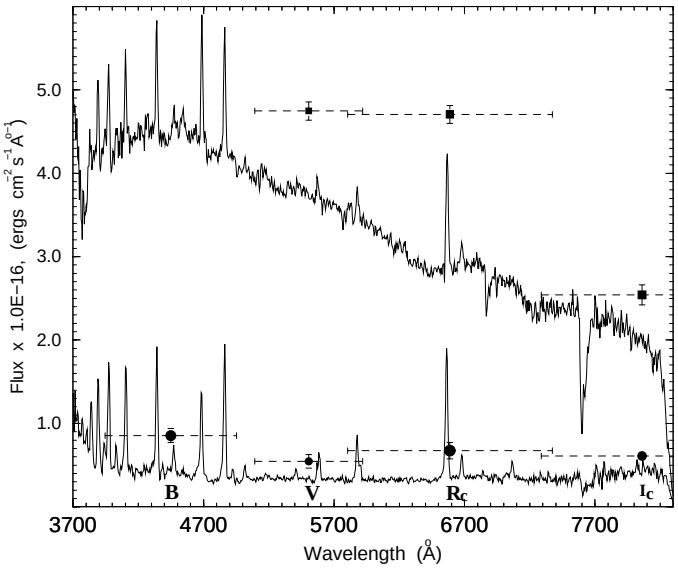

Fig. 7. Spectra of RX J0704.2+6203 at the top of the cyclotron hump and at the bottom.

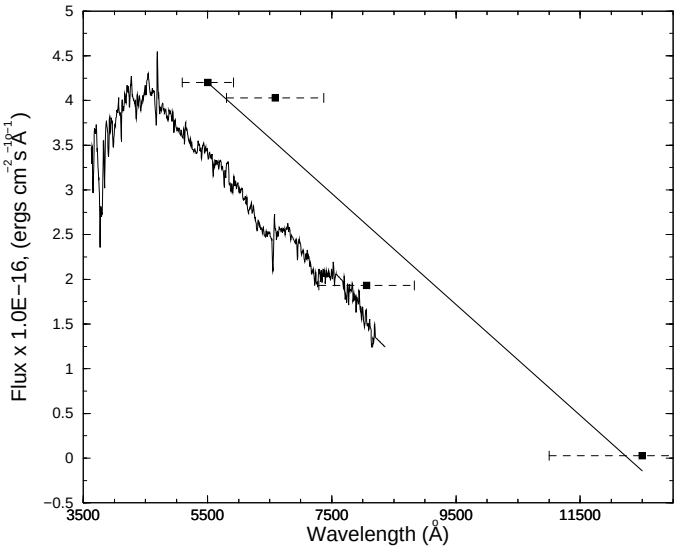

Fig. 8. Differential spectrum of RX J0704.2+6203 between the maximum and minimum in the light curve from spectrophotometric and photometric data (straight line). Cyclotron humps are clearly seen in the red part of the spectrum

of RV, as well as defined high and low luminosity states, is confirmed by direct estimate of the magnetic field of WD by fitting the cyclotron emission spectrum. We can go one step further and estimate other parameters of the system. ¿From the fact that the light curves show no eclipses, other than self eclipse of the accreting, magnetic pole by the WD itself, we can safely assume that the inclination of the system is less than $\approx 70°$. On the other hand we can measure substantial high velocities from the stream of transferred matter (upto 420 km/sec). At least the ballistic part of the stream should lie in or close to the orbital plane, thus the inclination of the system can not be very small, otherwise projected velocities would be much less than those observed in high inclination systems like HU Aquarii (Schwope et al. 1997) and RX J0719.2+6557 (Tovmassian et al. 1999). So we anticipate that the inclination of the system is not less than 30°. This in turn will lead to restrictions imposed on an angle β between the rotation axis and line of sight. The fact that the magnetic pole remains behind the limb of the WD during almost 0.6 orbital phase, as evident from the light curves, the angle β should be somewhere in between 120 and 150 degrees, as follows from the definition of the magnetic geometry by Cropper(1990).

5. Doppler tomography

Doppler tomography (Marsh & Horne 1988) is a technique that allows a determination of the velocity field of the matter in the orbital plane of close binary systems. It has been successfully applied in a number of studies of CVs and particularly magnetic systems (i.e. Schwope et al. 1997). Usually by providing orbital phases as a parameter for Doppler reconstruction, one obtains velocity maps or the images in a fixed coordinate system. Our examination of light curves and radial velocity curves failed to determine the orbital phases of the binary system. the absence of eclipses or any measurable contribution from the stellar components of the system prevents us from using common methods of phase determination. Nevertheless we performed Doppler tomography on our data using an arbitrary zero point for orbital phases. We used an optimized maximum entropy method (MEM; the code kindly provided by Spruit 1998). The resulting images clearly show the prolonged concentration of emission (matter), that is usually attributed to the stream from the donor secondary star to the WD (see for example Hoard et al. 1999). We estimated the zero point of orbital phases that placed the accretion stream at the usual location in the Doppler map. The corresponding inferior conjunction is at $T0 = 2451141.87 \pm 0.005$. Although the uncertainty of such a determination, based on eye inspection, is high (up to 0.1 orbital phase), its validity is out of doubt. Therefore, MEM Doppler maps confirm that the emission lines originate in the accretion stream, with the free-fall component being a major contributor. The resulting maps are presented in Figure 9 with corresponding observed and reconstructed trailed spectra of emission lines. Note the difference in velocities of He II and H_β! There is more emission coming from magnetic part of the stream in He II than in H_β. In H_β tomogram we actually see the main component of the emission line, coming from the balistic part, because it is much stronger than the second component. While in He II the second component has more contribution and easily could be traced by eye in the phase-folded trailed spectrum (between phases 1.0 – 1.5) as well as on the velocity map. It is seen as exten-

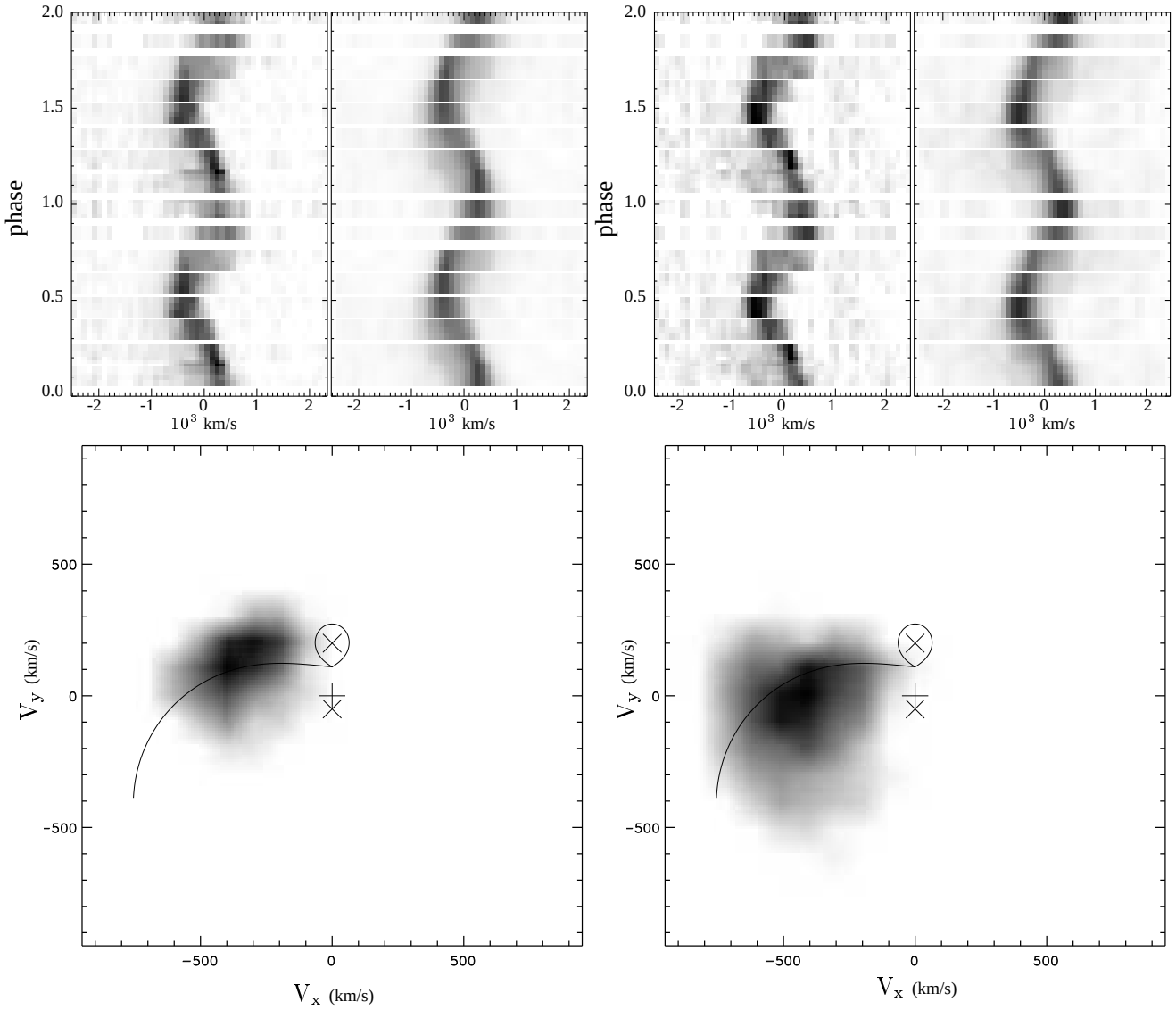

Fig. 9. The Doppler maps of the Hβ (left) and He II (right) emission lines of RX J0704.2+6203. The secondary star Roche lobe and ballistic accretion stream trajectory are plotted for an assumed inclination angle of 30°, primary mass M_1=0.7 and mass ratio $q = 0.25$. Above panels show phase folded observed and reconstructed trailed spectra of corresponding lines.

tion of the main spot towards negative V_y^1 velocities. For indication of Roche lobe of secondary, location of primary WD and the stream of matter in the map we selected reasonable binary parameters (the inclination angle of 30°, primary mass M_1=0.7 with mass ratio $q = 0.25$) to fit the observed characteristics of the stream.

The absence of evidence for secondary heating in RX J0704.2+6203 in the Doppler maps is noteworthy. The single spot on the maps clearly can not belong to the irradiated secondary due to its extremely high velocity and its elongated shape. This particular feature is another characteristic that makes RX J0704.2+6203 a twin of BL Hyi (Mennickent et al.1999), since the majority of AM Her systems show a significant contribution from the irradiated secondary in the line emission.

6. Conclusions

We found that the optical counterpart of X-Ray source RX J0704.2+6203 is a magnetic CV (AM Her type).

The orbital period of the system is 97 min and it increments the number of polars that are clustered around a 100 min peak.

The preliminary estimate of magnetic strength of probably dipole WD in the system is B=20-24 MG.

The system resembles the southern polar BL Hyi in its characteristics. The most striking similarity is that both

systems have no signs of an irradiated secondary star in their emission lines, unlike other AM Her objects. (Mennickent etal 1999)

our rough estimate of the inclination angle is $30 < i < 60$ and of the angle between the rotation axis and field vector is $120 < \beta < 150$.

Photometry obtained in low and high states shows that the magnetically driven accretion does not halt but reduces its magnitude at the low state. The reduction of cyclotron luminosity by ≈ 2 magnitudes leads to the conclusion that either accretion area or accretion rate decreases by a factor of 6.

The absence of secondary irradiation does not support speculations that the accretion rate changes could be the result of the heating of a part of that star.

Acknowledgements. GT is supported by CONACYT under grant 25454-A. PS acknowledges partial support from NASA LTSA grant NAG-53345. JG is supported by the Deutsche Agentur für Raumfahrtangelegenheiten (DARA) GmbH under contract FKZ 50 QQ 9602 3. The ROSAT project is supported by the German Bundesministerium für Bildung, Wissenschaft, Forschung und Technologie (BMBF/DARA) and the Max-Planck-Society.

References

Appenzeller, I., Thiering, I., Zickgraf, F.-J., Krautter, J., Voges, W., Chavarria, C., Kneer, R., Mujica, R., Pakull, M., Rosso, C., Ruzicka, F., Serrano, A., Ziegler, B., 1998 ApJS, 117, 319

Beuermann, K., and Burwitz, V., 1995, ASP Conf. Ser., 85, 99

Chanmugam, G., and Dulk, G.A., 1981, ApJ, 244, 569

Cropper, M., 1990, SSRv, 54, 195

Hoard, D.W. at Annapolis Workshop on Magnetic Cataclysmic Variables. ASP Conf. Ser., 157, 1999, eds. Hellier, C. and Mukai, K., p201.

Ferrario, L., Bailey, J., Wickramasinghe, D., 1996, MNRAS, 282, 218

Marsh, T.R., and Horne, K. 1988, MNRAS, 235, 269

Mennickent, R. E., Diaz, M. P., Arenas, J., 1999, A&A, 352, 167

Roberts, D. H., Lehar, J., Dreher, J. W., 1987, AJ, 93, 968

Schwope, A. D., Beuermann, K., Jordan, S., 1995, A&A, 301, 447

Schwope, A.D., 1996, Cataclysmic Variables and Related Objects, A. Evans and J.H. Wood (eds.), Kluwer, pp. 189

Schwope, A.D., Mantel, K.-H., Horne, K., 1997, A&A, 319, 894

Schwope, A.D., Schwarz, R., Staude, A. at Annapolis Workshop on Magnetic Cataclysmic Variables. ASP Conf. Ser., 157, 1999, eds. Hellier, C. and Mukai, K., p71.

Spruit H.C., 1998, astro-ph/9806141

Tovmassian, G. H.; Greiner, J.; Kroll, P.; Szkody, P.; Mason, P. A.; Zickgraf, F.-J.; Krautter, J.; Thiering, I.; Serrano, A.; Howell, S.; Ciardi, D. R., 1998 A&A, 335, 227

Tovmassian, G., Szkody, P., Greiner, J., Vrielmann, S., Kroll, P., Howell, S., Saxton, R., Ciardi, D., Mason, P.A., Hastings, N.C., 1999, Annapolis Workshop on Magnetic Cataclysmic Variables, ASP Conference Series, Volume 157, edited by Coel Hellier and Koji Mukai, p. 133

Tovmassian, G. H., Greiner, J., Schwope, A. D., Szkody, P., Schmidt, G., Zickgraf, F.-J., Serrano, A., Krautter, J., Thiering, I., Zharikov, S. V., 2000, ApJ, 537, 927

Warner, B., Cataclysmic Variable Stars, Cambridge University Press.

Wickramasinghe, D.T., Meggitt, S.M.A., 1985, MNRAS 214, 605

Wolff, M. T., Wood, K. S., Imamura, J. N., Middleditch, J., Steiman-Cameron, T.Y., 1999, ApJ, 526, 435

Zickgraf F.-J., Thiering I., Krautter J. Appenzeller I., Kneer R., Voges W.H., Ziegler B., Chavarria C., Serrano A., Mujica R., Pakull M., Heidt J., 1997, A&As, 123, 103